Front. Environ. Sci. Eng. 2022, 16(1): 10
https://doi.org/10.1007/s11783-021-1444-0

RESEARCH ARTICLE

Characterization and seasonal distribution of microplastics in the nearshore sediments of the south-east coast of India, Bay of Bengal

K. Dhineka, M. Sambandam, S. K. Sivadas, T. Kaviarasan, Umakanta Pradhan, Mehmuna Begum, Pravakar Mishra (✉), M. V. Ramana Murthy

National Centre for Coastal Research (NCCR), Ministry of Earth Science (MoES), Chennai 600100, India

HIGHLIGHTS

- MPs in the coastal sediment of south-east coast of India are quantified.
- High MPs are recorded near river mouths and nearshore regions.
- Polyethylene and polypropylene are the major polymers observed.
- MPs contamination is higher than the values reported elsewhere.

ARTICLE INFO

Article history:
Received 30 August 2021
Revised 25 November 2021
Accepted 28 November 2021
Available online 24 December 2021

Keywords:
Microplastics
Coastal sediment
Characterization
Bay of Bengal
India

GRAPHIC ABSTRACT

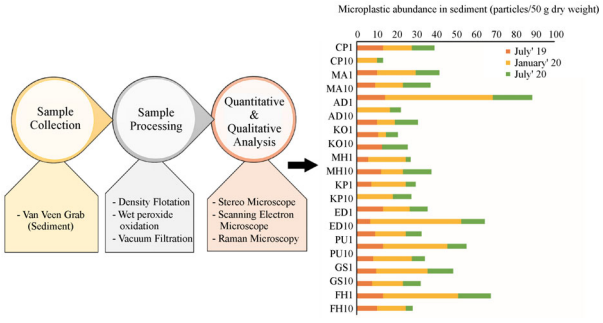

ABSTRACT

In view of increasing Microplastics (MPs) contamination in the marine environment and dearth of baseline data, a study was conducted on the abundance, characterization, and seasonal distribution of MPs in the nearshore sediments of the south-east coast of India. Sediment samples (n = 130) were collected at a distance of 1 km and 10 km from the shore region at varying depths (8–45 m) along the Chennai to Puducherry coast (165 km stretch), representing two seasons, i.e., south-west (July 2019 and July 2020) and north-east (January 2020) monsoons. The average abundance of MPs at the 22 offshore sites along the Chennai to Puducherry coast varied from 9±4.3 to 19±12.9 particles/50 g dry weight, in July 2019 and January 2020, respectively. July 2020 had an average abundance of 10±4.5 particles/50 g dry weight. Spatially, high levels of MPs were found at 1km stations and transects in proximity to the river inlets, and temporally, the north-east month recorded the maximum concentration. The dominant morphotype was the filament, and the major polymers were polyethylene and polypropylene. Scanning Electron Microscope (SEM) images revealed the surface irregularity and degradation of MPs due to weathering. The study highlights that high sediment contamination by MPs occurs during heavy rainfall and accumulates closer to river inlets. Eventually, this study suggests that appropriate management of plastic wastes on the landside will reduce MP contamination in the marine environment.

1 Introduction

Plastics have impacted almost every sphere of human life. The dearth of stringent regulations and inadequate plastic waste management and disposal are the primary reasons for the sharp increase in plastic litter observed over the past 60 years, from 1.7 million to over 320 million tons (Wright and Kelly, 2017). Coastal systems are highly vulnerable to both land and sea-based sources of plastic input. Plastics

✉ Corresponding author
E-mail: mishra@nccr.gov.in

Special Issue—Microplastic and Nanoplastic Pollution: Characterization, Transport, Fate, and Remediation Strategies (Responsible Editors: Wen Zhang, Melissa Pasquinelli & Yang Li)

may be beached, transported to the open ocean, or deposited on the seafloor, depending on their nature and the coastal system. MPs (size ranging 1μm to 5 mm) are solid particles, consisting of synthetic or heavily modified natural polymers as an essential ingredient, of primary or secondary origin, and insoluble at 20°C. (Hartmann et al., 2019). Based on its origin, MPs are classified into two types, (i) primary MPs that are factory-made, synthetic clothes, beads stitched or attached to personal care products etc. and (ii) secondary MPs that are formed as a result of degradation of larger plastic particles due to various physical and chemical factors (Cole et al., 2011).

The buoyant nature of MPs makes them easier to transport within aquatic and marine environments (Hidalgo-Ruz et al., 2012). The particles with a higher density (>1.02 g cm^{-3}) might sink faster, while those not as dense may reach the seafloor through density modification due to the encrustation of foulants (Andrady, 2011). On the hand, the size ranges of MPs account for the easier bioavailability of the lower trophic organisms (Naidu, 2019). The color variation of MPs also mimics the prey for marine predators, leading to adverse effects on these organisms (Shaw and Day, 1994). Apart from the intrinsic harm caused by monomers and additives (phthalates, flame retardants, etc.), the larger surface-to-volume ratio of MPs acts as an excellent adsorbent for trace metals and persistent organic pollutants which make them even more toxic (Andrady, 2011). Therefore, understanding the distribution of MPs in the coastal sediments is crucial in formulating feasible solutions for protecting the marine ecosystem. In addition to their vast numbers, the shape, size, distribution, color, and polymer type of the MPs should be considered as equally important factors to attain an appropriate risk assessment.

The number of research publications on MPs has increased over the last decade, but these have been more biased toward beach systems, as they are relatively easier to study. Nevertheless, a few studies have reported higher quantities of MPs in both offshore and deep-sea sediments (Zobkov and Esiukova, 2017; Peng et al., 2018). Studies on MPs in India focus more on beach systems, coastal surface water, and biota (Naidu, 2019; Jeyasanta et al., 2020). There is a marked paucity of information on the presence of MPs in the Indian coastal sediments.

The Indian coastal region is controlled by three seasons, *viz.,* south-west monsoon (June–September), north-east monsoon (October–January), and fair weather (February–May). The Bay of Bengal is influenced by current reversals, seasonal winds, and changes in precipitation. Cyclones frequently occur in the Bay of Bengal from October to January. The seasonal circulation patterns in the region are primarily controlled by wind and wave characteristics, and the resulting longshore sediment transport (littoral drift) is dominantly northward, within a few kilometers from the coastline. It is vital to trace the sources of MP contamination, its consequences, and its distribution patterns in the nearshore environment. Thus, in this context, the present study aims to analyze the characteristics and spatio-seasonal distribution of MPs in the coastal sediment of the south-western Bay of Bengal. The study has two main objectives *viz*., (i) to generate baseline data and (ii) to establish the linkage between the source and the sink.

2 Materials and methods

2.1 Study area

A total of 11 sections were selected covering a distance of 165 km from the metropolitan city of Chennai (13.0815°N, 80.2921°E) to Puducherry (11.8735°N, 79.8213°E). Chennai has a population of around 10.9 million whereas Puducherry (also known as Pondicherry), a major tourist town and an erstwhile French colony, has a population of around 0.83 million located along this coast. The detailed information on the study area, its physiographic characteristics, and sampling locations are provided in Table 1. The sites were selected based on the pollution due to urbanization, tourism, fishing activities, and sites proximal to the river and estuaries.

2.2 Sample collection

Three research surveys were carried out during July 2019 (CRV Sagar Purvi), January 2020 (RV Sagar Manjusha), and July 2020 (CRV Sagar Anveshika). Replicate sediment samples were collected using Van Veen grab technique (Palatinus et al., 2019) at each transect of 1 km and 10 km from the shore. From the collected sediment grab samples, the top 5 cm layer was scooped using a metallic spoon and stored in an aluminum container. The sampling depth ranged from 8 to 45 m. Samples were tightly packed and transported to the laboratory for further analysis.

2.3 Extraction of MPs

The sediment samples were dried at 50°C in the hot air oven, until they were dried completely, and then processed for MP extraction (Zhao et al., 2018). A quantity of 50 g dried sediment sample was mixed with 200 mL pre-filtered saturated NaCl (ρ = 1.2 g/mL) solution and stirred for about 5 to 10 min. Subsequently, the solution was allowed to settle for about 10 to 15 min; next, the supernatant was transferred to a clean conical flask. This procedure was repeated thrice, to enhance the maximum recovery of MPs. For digestion of organic matter, 5 to 15 mL of 30% hydrogen peroxide solution was added to the supernatant and allowed to stay for 24 h. The supernatant was filtered through GF/F filter paper (pore size 0.7 μm) using vacuum filtration. The saturated saline solution used for analysis was prepared using distilled water, followed by filtration

Table 1 Study area description and the details of sampling.

Stations (code) with Geographical position	Parameter	July 2019		January 2020		July 2020		Characteristics of the stations
		1 km	10 km	1 km	10 km	1 km	10 km	
Chennai port (CP) 13.1172°N, 80.3154°E 13.1110°N, 80.3954°E	Depth (m) Sample (n)	16 2	28 *	19 2	28 2	15 2	27 2	Largest gateway hub port for Containers, Cars and Project Cargo on the East Coast of India, located in between the Cooum River (length = 65 km) and the Kasimedu fishing harbour.
Marina (MA) 13.0370°N, 80.2923°E 13.0184°N, 80.3718°E	Depth (m) Sample (n)	13 2	21 2	13 2	33.3 2	12 3	22 2	The longest urban beach in the country, known for its tourism, and has two river inputs Cooum River (north) and Adyar River (south).
Adyar (AD) 13.0104°N, 80.28868°E 12.9889°N, 80.3678°E	Depth (m) Sample (n)	11.5 2	25 *	13 2	31 2	13 2	35 2	Adyar River, 43 km long, joins the Bay of Bengal at the Adyar estuary, where boating and fishing activities takes place.
Kovalam (KO) 12.7957°N, 80.2598°E 12.7774°N, 80.3415°E	Depth (m) Sample (n)	12 2	38.5 2	11 2	45 2	8 3	43 1	Fishing village, where surfing takes place. Buckingham Canal, 4 km long is on the north side of the station, which discharges into the Kovalam Estuary.
Mahabalipuram (MH) 12.6129°N, 80.2090°E 12.5890°N, 80.2884°E	Depth (m) Sample (n)	11 2	39 2	13 *	42 2	11 2	41 2	Best known for the UNESCO's World Heritage Site, a famous tourist spot in India.
Kalpakkam (KP) 12.5570°N, 80.1883°E 12.5310°N, 80.2670°E	Depth (m) Sample (n)	12 2	36 2	11 2	38 2	11 2	36 2	The south side of Kalpakkam has a seasonal river of 350 km length (Palar River).
Edaikazhinadu (ED) 12.2817°N, 80.0311°E 12.2499°N, 80.1078°E	Depth (m) Sample (n)	10.5 *	25 2	10 2	26 2	8.5 3	26 2	It is situated between two backwaters i.e., Odiyur backwater on the north side and the Kaliveli lake joining the Edierthittu estuary.
Pondicherry University (PU) 11.9720°N,79.8544°E 11.9498°N,79.9340°E	Depth (m) Sample (n)	11 2	22 2	10.6 1	25 2	9 3	25 3	Near the sampling station of Pondicherry University, Auroville (international village) beach is located. It is an important tourist destination for both local and international travelers.
Gandhi statue (GS) 11.9292°N,79.8452°E 11.9089°N,79.9250°E	Depth (m) Sample (n)	11 2	27 2	11 2	28.5 2	12 3	27 3	An important tourist destination in Puducherry attracting tourists throughout the year. North side of the beach receives untreated sewage from the town through a small channel.
Fishing harbour (FH) 11.9035°N,79.8400°E 11.8818°N,79.9196°E	Depth (m) Sample (n)	11 2	28.5 2	10.9 2	29 2	7 2	26 3	The hinterland of the sampling location has mangrove and backwaters of an estuarine system. The estuary receives untreated sewage from the adjacent town. A fishing harbour is located in the area.
Paradise Beach (PB) 11.8695°N,79.8321°E 11.8447°N,79.9089°E	Depth (m) Sample (n)	11 2	30 2	11 2	31 2	10 2	28 2	Paradise Beach is at 8 km south of Pondicherry town and has a fish landing center and known for turtle nesting ground. A small river of 75 km length drains into Bay of Bengal near this beach.

Note: * Samples could not be collected.

through GF/F filter paper, to prevent contamination. Before the analysis, all the glass beakers and conical flasks were rinsed with distilled water. Three procedural blanks were maintained to check the external contaminants and the analysis was carried out in an enclosed environment, and cotton attire was worn during the analysis.

2.4 Quantitative analysis

The quantification of MPs (Hidalgo-Ruz et al., 2012) was done using an RSMr series stereo zoom microscope. The morphotype of the MPs was categorized into three shapes: fragment, filament, and film. Based on the size (μm), MPs were clustered into ten groups (1–500, 501–1000, 1001–1500, 1501–2000, 2001–2500, 2501–3000, 3001–3500, 3501–4000, 4001–4500 and 4501–5000) (Zhao et al., 2018). The color categories of MPs included black, blue, red, yellow, white, and transparent (Peng et al., 2017). The MP particles were reported per 50 g dry weight (d.w.). Sediment texture analyses were made following a standard protocol to correlate with MP concentration (Folk and Ward,1957).

2.5 Qualitative analysis

Raman microscope spectroscopy (Renishaw) coupled with a confocal microscope (50 × and 100 × objectives) was used for polymer identification. The Raman shift was calculated at an excitation wavelength of 532 nm, covering the spectral frequency of 100 cm^{-1} to 3500 cm^{-1}. Scanning Electron Microscopy (SEM) – JSM-IT500 (version 1.110) was performed to understand the MPs' surface morphology and weathering pattern. The selected MP samples were mounted on a metal stub, using a double-sided adhesive carbon tape. Subsequently, the specimen was sputter-coated with a fine layer of gold, using D11-29030SCTR Smart Coater for 2 min.

2.6 Data analysis

Differences between the total number of particles and morphotype of plastics in the sediment were determined using a Two-Way Analysis of Variance (ANOVA) followed by Tukey's post-hoc test. Non-parametric Spearman correlation analysis was performed to determine the relationship between sediment grain size and MPs accumulation using STATISTICA 12 software.

3 Results

3.1 MP abundance and distribution

Spatially, the highest MPs concentration (14 particles/50 g d.w. in July 2019, 55 particles/50 g d.w. in January 2020, and 20 particles/50 g d.w. in July 2020) was recorded at Adyar 1 km (Fig. 1). Seasonally, the MPs contamination was the highest during January 2020 (19±12.9 particles/50 g d.w.) followed by July 2020 (10±4.5 particles/50 g d.w.) and July 2019 (9±4.3 particles/50 g d.w.). There was a sharp rise in the MP concentration from July 2019 to January 2020, which dropped during July 2020. Two-way ANOVA detected significant seasonal and spatial variability in the abundance of total MPs (Table 2). Tukey's post- hoc confirmed a significantly higher abundance of MPs during January 2020. It was observed that the MPs accumulation varied spatially and temporally; it was higher mainly throughout the southern transects (Pondicherry University to Paradise Beach), except for the Adyar station located in the northern transect.

For the 1 km stations, the total abundance of MPs ranged from 4 (Pondicherry University) to 14 particles/50 g d.w. (Adyar) in July 2019, 9 (Kovalam) to 54.5 particles/50 g d.w. (Adyar) during January 2020, and 9.33 (Edaikazhinadu) to 20 particles/50 g d.w. (Adyar) in July 2020, respectively. The abundance of MPs at 10 km ranged from 5.5 (Mahabalipuram) to 13 particles/50 g d.w. (Edaikazhinadu) in July 2019, 4 (Kovalam) to 19.5 particles/50 g d.w. (Gandhi Statue) in January 2020, and 2.5 (Mahabalipuram) to 14 particles/50 g d.w. (Marina) during July 2020.

3.2 Shape of MPs

Three different shapes of MPs were observed, as shown in Fig. 2. During July 2019, fragments (43%) were the dominant type, followed by filaments (35%) and films (22%) (Fig. 3(a)). The fragment range was between 1 and 25 particles/50 g d.w., with significant differences among the stations and seasons. However, Tukey's post-hoc test indicated significantly higher fragments recorded at Adyar-1 km, during January 2020. Furthermore, the abundance of filaments showed a significant difference at the seasonal level but not among the stations. Films displayed a similar trend as fragments, showing significant differences both spatially and seasonally (Table 2). Tukey's post-hoc test detected significantly higher values at Gandhi Statue 1 km, during January 2020. During July 2019, the MP abundance was in the range of 6 to 14 particles/50 g d.w.

A similar trend was observed in January 2020, wherein fragments (41%) dominated the MPs type, followed by filaments (35%) and films (24%) (Table 3). The fragments ranged from 1 to 39 (8.3±9.5) particles/50 g d.w., filaments from 2 to 14 (7.3±3.1) particles/50 g d.w., and films varied from 1 to 13 (4.8±3.2) particles/50 g d.w. The highest number of fragments was observed in Adyar 1 km and Paradise Beach 1 km, while the least number was at Chennai Port 1 km. Pondicherry University 1 km had a greater number of filaments, while Gandhi Statue 1 km had a greater number of films.

During July 2020, there was a slight deviation in the order of distribution i.e., filaments>fragments>films. Filaments contributed to more than half of the morphotype

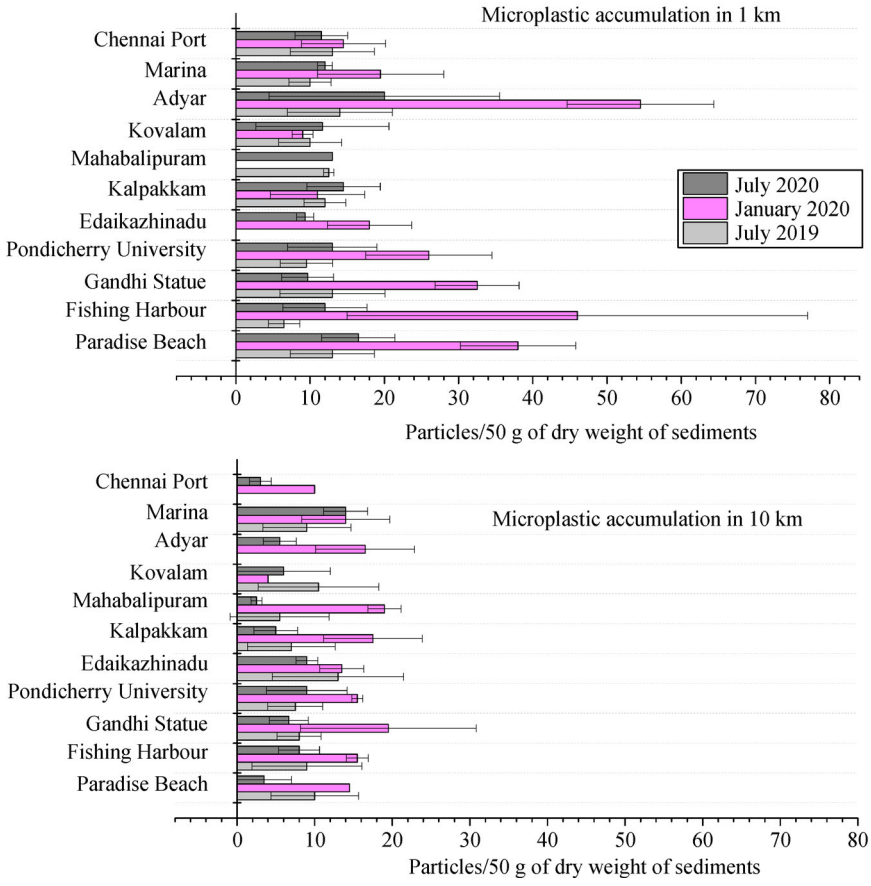

Fig. 1 Spatial and seasonal variation of microplastics observed in the Chennai–Puducherry coastal sediment.

Table 2 Two-Way Analysis of Variance (ANOVA) results showing significant differences in seasonal and spatial variability

Variable	Factor	Sum of Squares (SS)	Degrees of freedom (DF)	Mean Square (MS)	F-Value	P-Value
Total	Month	1150.51	2	575.25	18.28	0.00
	Station	1794.57	21	85.46	2.72	0.00
	Month × Stations	1215.66	38	31.99	1.03	0.45
Fragment	Month	97.93	2	48.96	4.41	0.01
	Station	682.18	21	32.48	2.93	0.00
	Month × Stations	663.22	38	17.45	2.31	0.00
Filament	Month	293.81	2	146.90	11.57	0.00
	Station	233.38	21	11.11	0.88	0.62
	Month × Stations	578.66	38	15.23	1.35	0.14
Film	Month	277.03	2	138.51	41.26	0.00
	Station	146.72	21	6.99	2.08	0.01
	Month × Stations	193.99	38	5.11	2.15	0.00

Note: Values in bold are significant, $p < 0.05$; No of samples, $n = 130$.

ratio at about 59%, followed by fragments (34%) and films (7%), with values ranging from 1 to 13 (3.3±2.4) particles/50 g d.w., 1–7 (5.8±2.9) particles/50 g d.w., and 1–3 (0.7±0.8) particles/50 g d.w., respectively. The overall increase in the filament type is attributed mainly to Adyar 1 km and Paradise Beach 1 km, which changed the pattern of morphotype distribution when compared to the two other months. Fragments were more prevalent at Pondicherry University 1 km, while films were dominant at the Adyar 1 km station.

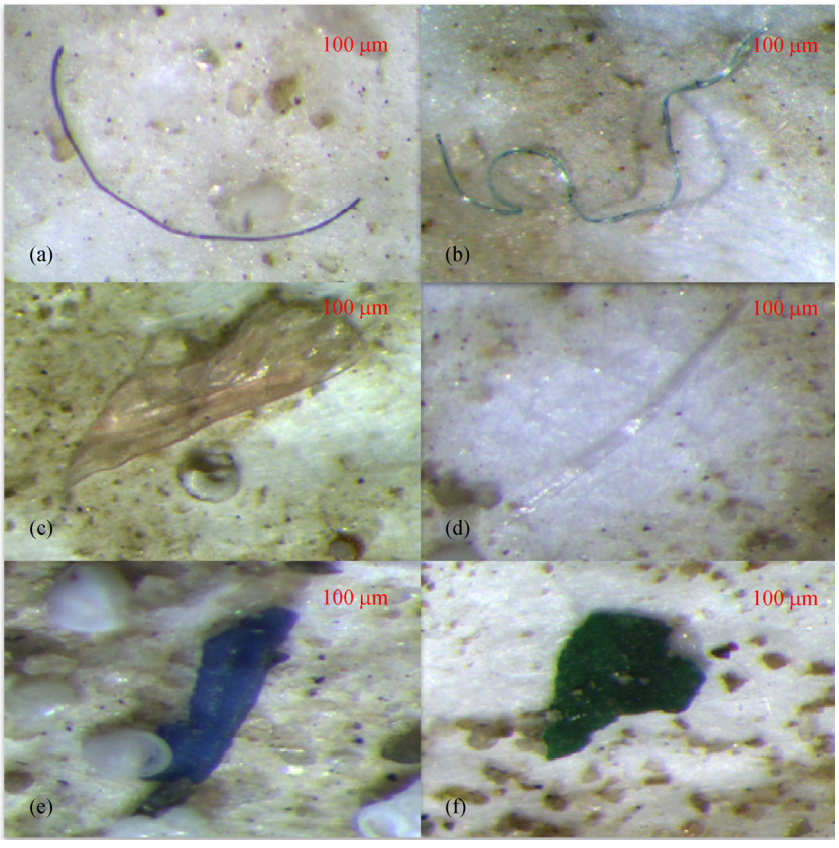

Fig. 2 Microscopic images of microplastics (a) & (b) filaments; (c) & (d) films; (e) & (f) fragments.

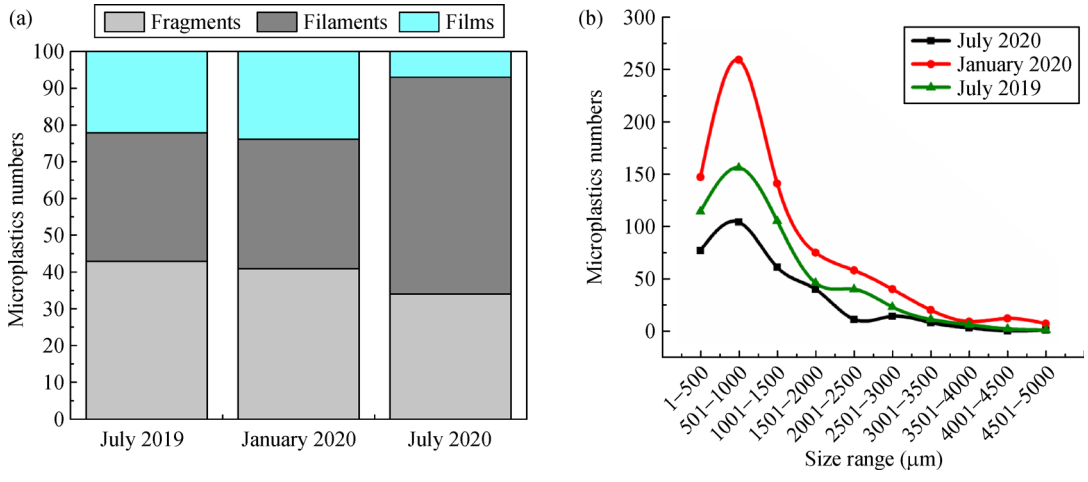

Fig. 3 (a) Morphotype composition, (b) Size range comparison of the microplastics.

3.3 Size of MPs

The maximum number of MPs for all three sampling periods was in the size range of 501–1000 μm, followed by 1–500 μm and 1001–1500 μm. The least number of MPs were in the size class of 4501–5000 μm. The percentages of MPs in the size class of 501–1000 μm were 32.6%, 33.72%, and 30.95%, for July 2019, January 2020, and July 2020, respectively (Fig. 3(b)). Class sizes between 2001 and 5000 μm contributed to $< 20\%$ of the total abundance of MPs. Another interesting finding is that the size class (501–1000 μm) of MPs was found to be dominant in both the 1 km and 10 km stations, respectively, all the seasons.

Sediment grain size analysis indicates that sand was dominant in all the seasons (July 2019: 90%–100%, January 2020: 89%–100%, July 2020: 89%–100%) except for four stations of 10 km. Spearman's correlation analysis did not establish any relationship between the grain size and MP concentration.

3.4 Color of MPs

MPs of six different colors (white, blue, transparent, yellow, black, and red) were observed (Fig. 4). The most common color during July 2019 and July 2020 was blue (26% and 29%), whereas, in January 2020, it was transparent (30%).

3.5 Qualitative analysis

Spectroscopic results (Fig. 5) revealed four common polymer types (polyethylene-PE, polypropylene-PP, polyvinyl chloride-PVC, polyamide-PA). The polymer identification was validated using the published literature (Liu et al., 2020). For PE, relatively weaker peaks were observed around 2846–2881 cm^{-1} while a broader and strong band was seen in the range of 2100–2200cm^{-1}. PP was identified by the several peaks at 2800–3000 cm^{-1} caused by the CH2 stretching vibration. The CH2 stretching vibration at around 2914 cm^{-1} represents the PVC, while the CH(CH2) stretching at 2871 to 2943 cm^{-1} indicates the presence of PA. The high

Table 3 Average abundance and shape distribution (%) of microplastics in the Bay of Bengal Coast (Chennai-Puducherry)

S. No.	Period	Fragments	Filaments	Films
MP Average abundance (Particles/50 g Dry weight)				
1	July, 2019	4.4±1.4	3.6±1.9	2.2±1.4
2	January, 2020	8.3±9.5	7.3±3.1	4.8±3.2
3	July, 2020	3.3±2.4	5.8±2.9	0.7±0.8
Shape distribution (%)				
4	July, 2019	43	35	22
5	January, 2020	41	35	24
6	July, 2020	34	59	7

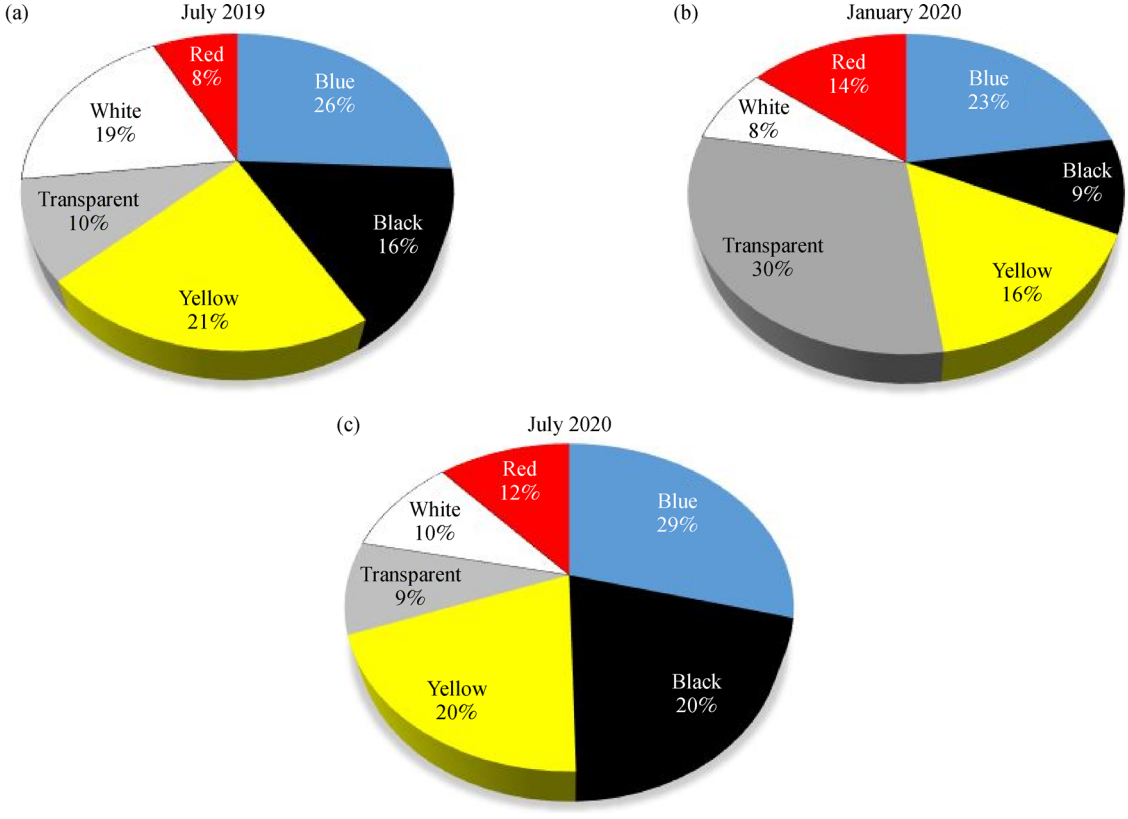

Fig. 4 Percentage of microplastic colors at (a) July 2019, (b) January 2020, and (c) July 2020.

magnification SEM images depict the multiple layers of MPs with a rough surface and rupture at the edges, as shown in Fig. 6. The fractures and roughness patterns indicate the prolonged exposure of MPs in the marine environment, which are subjected to various degradation processes.

4 Discussion

The study area located on the south-western coast of the Bay of Bengal is primarily influenced by the south-west monsoon (SWM) and the north-east monsoon (NEM). During the SWM, the East Indian Coastal Current (EICC) moves northward, while it moves toward the equatorial region, during the NEM. In the present study, MPs accumulation was found to be higher during the NEM. Similarly, Veerasingam et al., 2016a also observed higher levels of MPs in the NEM than in the SWM, along the high tide line of the Chennai coast. The coastal water circulation patterns seem to affect the transport of contaminants and waste disposal (Zhang et al., 2020).

Rivers are considered to be the potential carriers of MPs, estimated to transport about 91% of the mismanaged plastic waste to the ocean (Lebreton and Andrady, 2019). Precipitation plays a crucial role in MP transport among coastal habitats (Zhu et al., 2018). Chennai registered maximum rainfall during October- December 2019. In general, the freshwater discharge of the Adyar River is higher than the annual mean during the NEM (Rajkumar et al., 2008), which explains the higher MP abundance recorded in the Adyar station during all the seasons, especially during the NEM. Furthermore, the discharge of the Adyar and Cooum rivers was found to influence the higher MPs accumulation recorded at the Marina beach (Sathish et al., 2019).

The southern transect (Puducherry) has a higher MP concentration than the northern transect (Chennai) since the regional runoff, tide, current, and salinity may influence the spatial distribution of MPs (Yu et al.,

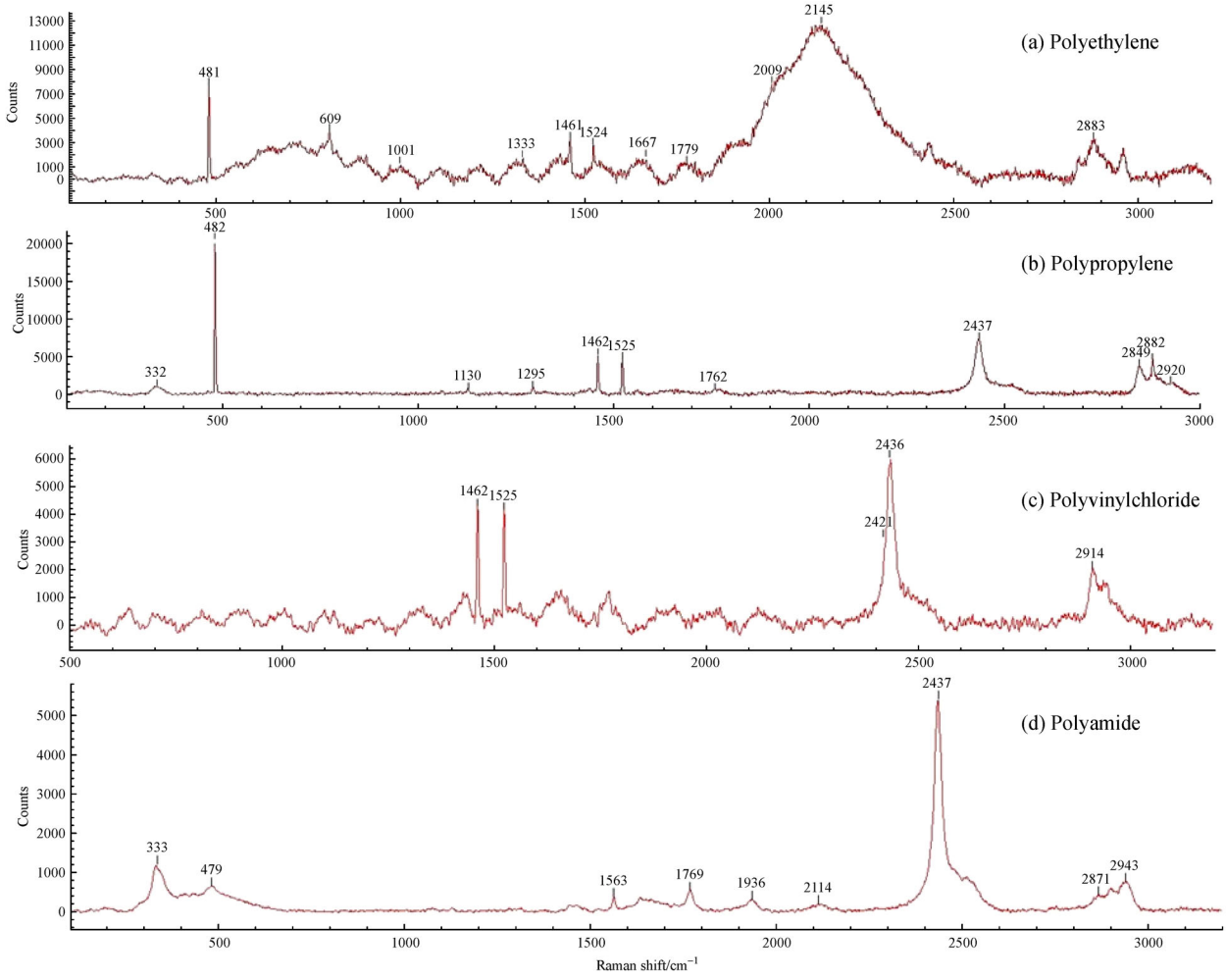

Fig. 5 Raman spectra of the polymer microplastics (a) Polyethylene, (b) Polypropylene, (c) Polyvinylchloride, and (d) Polyamide.

2018). Also, tourist beaches in Puducherry involve human activities (direct emission of plastics disposal), weathering degradation of these plastics on the beaches results in their surface embrittlement and micro-cracking, yielding micro-particles that are carried into the water by wind or wave action resulting in the plastic debris being swept away into the ocean by tides and currents (Andrady, 2011). This debris eventually reaches the seafloor sediments. Additionally, fishing activities were found to be the major cause of the high level of MPs on the Puducherry beaches (Dowarah and Devipriya, 2019).

The average MP concentration during each period, as observed in the present study, was compared with the few other reports published worldwide. To enable comparison with earlier published reports, all the units were converted into particles/kg d.w. The MPs abundance in our study is several magnitudes higher than the other locations across world oceans (Table 4) (Graca et al., 2017; Zobkov and Esiukova, 2017; Zhao et al., 2018; Mu et al., 2019). Despite the difference in MPs levels, all these studies reported higher levels near the river mouth stations (e.g., Vistula River outlet in Polish Coast of Baltic Sea; river mouths of the Mackenzie and Colville in the Northern Bering and Chukchi Sea), and also toward the landward sites. This corresponds to our findings. It is interesting to note that, size ranging less than 2 mm is found to be dominant in all these studies. Also, there is a decline in the concentration of MPs as the distance from the nearshore to offshore regions increases (Graca et al., 2017). Another study also showed that the size and density of the marine debris increased from the coastal waters to the backshore regions (Olivelli et al., 2020). This corroborates the fact that MPs distribution is lesser at 10 km stations than the 1 km stations.

Concerning the morphotype, fragments were dominant in July 2019 and January 2020, followed by filaments and films. On the other hand, filaments prevailed in July 2020, followed by fragments and films. Fragments and filaments (fibers) are the most common shapes of MPs observed in the Indian coastal sediments (Dowarah and Devipriya, 2019) and other regions of the world (Graca et al., 2017; Mu et al., 2019), due to their higher density and lower specific surface area, leading to easier deposition in the sediments (Lin et al., 2018). Fragments are found as a result of degradation of macro (>2.5 cm) and meso (5 mm to 2.5 cm) plastics (Free et al., 2014), while fishing activities and sewage (synthetic fibers through washing clothes) pave the way for filaments (Zhao et al., 2018; Zhu et al., 2018), which could be the possible sources of MPs.

In terms of the size range, the maximum number of MPs lies within the range of 501–1000µm followed by 1–500 µm, similar to the previous studies, which proved that smaller size MPs are present profusely on the seafloor sediments (Nor and Obbard, 2014; Peng et al., 2017; Zhao et al., 2018). Thus, there is a possibility that the smaller MPs from the freshwater bodies can be transported into the marine environment, which attributes to the prevalence of smaller-sized MPs, even at the 1 km stations. Temporally, there is no significant difference in the size range of MPs. Size plays a vital role in facilitating the biological impact of MPs. This was demonstrated in a study by Ziajahromi et al., 2018 on how different sizes of MPs had detrimental effects on the blood worm (*Chironomus tepperi*). Most importantly, the presence of smaller-sized MPs in the sediment-associated biota *Perna viridis*, which was collected from the Chennai coast, was reported by Naidu, 2019. This explains the fact that these smaller-sized MPs have been ingested by the biota.

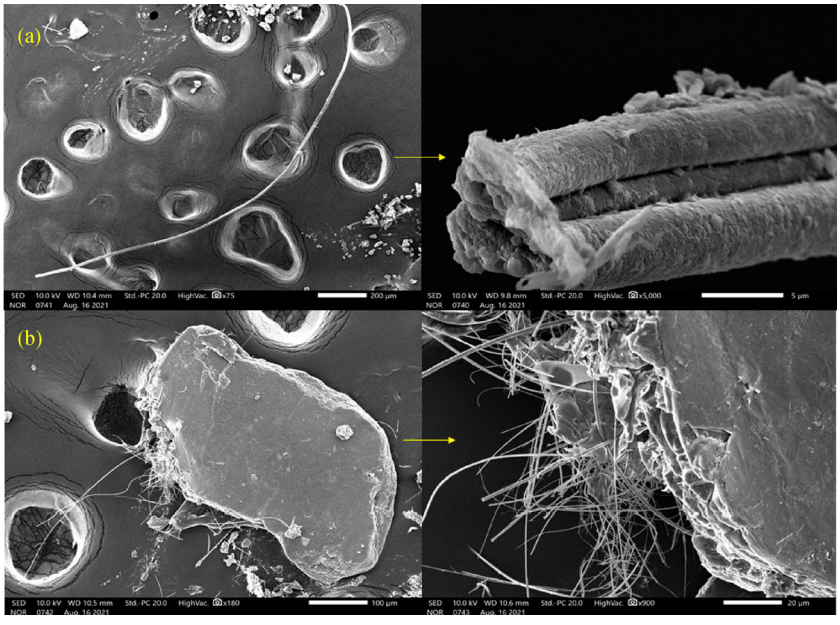

Fig. 6 Scanning Electron Microscopy images of microplastics (a) filament, and (b) fragment.

Table 4 Abundance of microplastics in the sediments from various regions

S. No.	Location	No. of samples (n)	Abundance	Reference
1	Baltic Sea, Russia	7	34±10 items/kg d.w.	Zobkov and Esiukova, 2017
2	Southern Baltic Sea	14	0 to 27 particles/kg d.w.	Graca et al., 2017
3	China	216	171.8 items/kg (Bohai sea) 123.6 items/kg (Northern Yellow Sea) 72.0 items/kg (Southern yellow sea)	Zhao et al., 2018
4	Northern Bering and Chukchi Seas	7	ND ~ 68.78 items/kg d.w.	Mu et al., 2019
5	South-east coast of India, Bay of Bengal	130	175±85 particles/kg d.w. (July 2019) 390±260 particles/kg d.w. (January 2020) 196±91 particles/kg d.w. (July 2020)	Present study

Color plays a vital role in MP analysis, since it is helpful for the possible source identification of the plastic debris (Veerasingam et al., 2016b; Hartmann et al., 2019), and has a greater influence on the bioavailability of marine organisms (Naidu, 2019). Blue is commonly observed (Peng et al., 2017), followed by transparent and yellow. Transparent MPs are observed more in ray-finned fishes (Zhu et al., 2019) and blue ones in longer sunfish (Peters and Bratton, 2016). This explains the MP life cycle inside the marine ecosystem and the transportation between the matrices i.e., from coastal sediment to marine biota. Discoloration of MPs was observed at a few stations, which indicates that severe weathering processes have occurred due to the presence of additives (e.g., phenolic antioxidants) (Acosta-Coley and Olivero-Verbel, 2015). Spearman's correlation analysis showed that the grain-size did not positively correlate with the MP distribution (Nor and Obbard, 2014). The presence of lower density polymers i.e., polyethylene and polypropylene confirm that the majority of the MPs reached the sediment layer due to the biofouling effect (Andrady, 2011). Thermoplastics, namely polyethylene, and polypropylene, are the principal plastic materials recovered from the sewage treatment plant (Kang et al., 2018). It is evident from the SEM analysis that a large quantity of MPs is released from a single plastic fragment. Mechanical and/or biological degradation processes are responsible for the ruptures of plastic fragments and the disintegration of the MPs (Zhou et al., 2018).

5 Conclusions

The present study on distribution and characterization of the MPs in the nearshore sediment indicates that transects closer to the river inlets had higher concentrations, thereby indicating that the source of pollution is land-based. Anthropogenic activities such as sewage discharge, and fishing are the major contributing factors for MP contamination in the region. Based on the plastic-type, it is apparent that most of them have originated from packaging materials, disposed of in the open. Under the Extended Producer's Responsibility (EPR), manufacturers of packaging industries should be made responsible for monitoring and controlling plastic waste. Since the riverine input acts as a significant pathway for pollution, cleaning technologies like trash barriers or trash skimmers can be employed at the river mouths to remove the floating plastic litter. The level of MPs pollution is relatively higher than reported elsewhere, demanding immediate attention toward formulating feasible solutions to address the MPs pollution along the south-east coast of India.

Acknowledgements The authors are grateful to the Secretary, Ministry of Earth Sciences, Government of India for their support and encouragement. We are thankful to Dr. V Sampath for critically going through the manuscript and the Captain and crew of Research Vessels for their help during the collection of samples. This work is an output of the Marine Litter and Microplastic program of NCCR with contribution number NCCR/16/2019/MS-370. The funding source of this study is Ministry of Earth Sciences, Government of India.

References

Acosta-Coley I, Olivero-Verbel J (2015). Microplastic resin pellets on an urban tropical beach in Colombia. Environmental Monitoring and Assessment, 187–435

Andrady A L (2011). Microplastics in the marine environment. Marine Pollution Bulletin, 62(8): 1596–1605

Cole M, Lindeque P, Halsband C, Galloway T S (2011). Microplastics as contaminants in the marine environment: A review. Marine Pollution Bulletin, 62(12): 2588–2597

Dowarah K, Devipriya S P (2019). Microplastic prevalence in the beaches of Puducherry, India and its correlation with fishing and tourism/recreational activities. Marine Pollution Bulletin, 148: 123–133

Folk R L, Ward W C (1957). Brazos River bar [Texas]; a study in the significance of grain size parameters. Journal of Sedimentary Research, 27(1): 3–26

Free C M, Jensen O P, Mason S A, Eriksen M, Williamson N J, Boldgiv B (2014). High-levels of microplastic pollution in a large, remote, mountain lake. Marine Pollution Bulletin, 85(1): 156–163

Graca B, Szewc K, Zakrzewska D, Dołęga A, Szczerbowska-Boruchowska M (2017). Sources and fate of microplastics in marine and beach sediments of the Southern Baltic Sea: A preliminary study. Environmental Science and Pollution Research International, 24(8):

7650–7661

Hartmann N B, Huffer T, Thompson R C, Hassellöv M, Verschoor A, Daugaard A E, Rist S, Karlsson T, Brennholt N, Cole M, Herrling M P, Hess M C, Ivleva N P, Lusher A L, Wagner M (2019). Are we speaking the same language? Recommendations for a definition and categorization framework for plastic debris. Environmental Science & Technology, 53(3): 1039–1047

Hidalgo-Ruz V, Gutow L, Thompson R C, Thiel M (2012). Microplastics in the marine environment: A review of the methods used for identification and quantification. Environmental Science & Technology, 46(6): 3060–3075

Jeyasanta K I, Sathish N, Patterson J, Edward J P (2020). Macro-, meso- and microplastic debris in the beaches of Tuticorin district, Southeast coast of India. Marine Pollution Bulletin, 154: 111055

Kang H J, Park H J, Kwon O K, Lee W S, Jeong D H, Ju B K, Kwon J H (2018). Occurrence of microplastics in municipal sewage treatment plants: A review. Environmental Health and Toxicology, 33(3): e2018013–8

Lebreton L, Andrady A (2019). Future scenarios of global plastic waste generation and disposal. Palgrave Communications, 5(1): 6

Lin L, Zuo L Z, Peng J P, Cai L Q, Fok L, Yan Y, Li H X, Xu X R (2018). Occurrence and distribution of microplastics in an urban river: A case study in the Pearl River along Guangzhou City, China. Science of the Total Environment, 644: 375–381

Liu J, Zhang X, Du Z, Luan Z, Li L, Xi S, Wang B, Cao L, Yan J (2020). Application of confocal laser Raman spectroscopy on marine sediment microplastics. Journal of Oceanology and Limnology, 38(5): 1502–1516

Mu J, Qu L, Jin F, Zhang S, Fang C, Ma X, Zhang W, Huo C, Cong Y, Wang J (2019). Abundance and distribution of microplastics in the surface sediments from the northern Bering and Chukchi Seas. Environmental Pollution, 245: 122–130

Naidu S A (2019). Preliminary study and first evidence of presence of microplastics and colorants in green mussel, *Perna viridis* (Linnaeus, 1758), from southeast coast of India. Marine Pollution Bulletin, 140: 416–422

Nor N H, Obbard J P (2014). Microplastics in Singapore's coastal mangrove ecosystems. Marine Pollution Bulletin, 79(1–2): 278–283

Olivelli A, Hardesty B D, Wilcox C (2020). Coastal margins and backshores represent a major sink for marine debris: insights from a continental-scale analysis. Environmental Research Letters, 15(7): 074037

Palatinus A, Kovač Viršek M, Robič U, Grego M, Bajt O, Šiljić J, Suaria G, Liubartseva S, Coppini G, Peterlin M (2019). Marine litter in the Croatian part of the middle Adriatic Sea: Simultaneous assessment of floating and seabed macro and micro litter abundance and composition. Marine Pollution Bulletin, 139: 427–439

Peng G, Zhu B, Yang D, Su L, Shi H, Li D (2017). Microplastics in sediments of the Changjiang Estuary, China. Environmental Pollution, 225: 283–290

Peng X, Chen M, Chen S, Dasgupta S, Xu H, Ta K, Du M, Li J, Guo Z, Bai S (2018). Microplastics contaminate the deepest part of the world's ocean. Geochemical Perspectives Letters, 9: 1–5

Peters C A, Bratton S P (2016). Urbanization is a major influence on microplastic ingestion by sunfish in the Brazos River Basin, Central Texas, USA. Environmental Pollution, 210: 380–387

Rajkumar A N, Barnes J, Ramesh R, Purvaja R, Upstill-Goddard R C (2008). Methane and nitrous oxide fluxes in the polluted Adyar River and estuary, SE India. Marine Pollution Bulletin, 56(12): 2043–2051

Sathish N, Jeyasanta K I, Patterson J (2019). Abundance, characteristics and surface degradation features of microplastics in beach sediments of five coastal areas in Tamil Nadu, India. Marine Pollution Bulletin, 142: 112–118

Shaw D G, Day R H (1994). Colour-and form-dependent loss of plastic micro-debris from the North Pacific Ocean. Marine Pollution Bulletin, 28(1): 39–43

Veerasingam S, Mugilarasan M, Venkatachalapathy R, Vethamony P (2016a). Influence of 2015 flood on the distribution and occurrence of microplastic pellets along the Chennai coast, India. Marine Pollution Bulletin, 109(1): 196–204

Veerasingam S, Saha M, Suneel V, Vethamony P, Rodrigues A C, Bhattacharyya S, Naik B G (2016b). Characteristics, seasonal distribution and surface degradation features of microplastic pellets along the Goa coast, India. Chemosphere, 159: 496–505

Wright S L, Kelly F J (2017). Plastic and human health: A micro issue? Environmental Science & Technology, 51(12): 6634–6647

Yu X, Ladewig S, Bao S, Toline C A, Whitmire S, Chow A T (2018). Occurrence and distribution of microplastics at selected coastal sites along the south eastern United States. Science of the Total Environment, 613– 614: 298–305

Zhang W, Zhang S, Zhao Q, Qu L, Ma D, Wang J (2020). Spatio-temporal distribution of plastic and microplastic debris in the surface water of the Bohai Sea, China. Marine Pollution Bulletin, 158: 111343

Zhao J, Ran W, Teng J, Liu Y, Liu H, Yin X, Cao R, Wang Q (2018). Microplastic pollution in sediments from the Bohai Sea and the Yellow Sea, China. Science of the Total Environment, 640-641: 637–645

Zhu L, Bai H, Chen B, Sun X, Qu K, Xia B (2018). Microplastic pollution in North Yellow Sea, China: Observations on occurrence, distribution and identification. Science of the Total Environment, 636: 20–29

Zhu L, Wang H, Chen B, Sun X, Qu K, Xia B (2019). Microplastic ingestion in deep-sea fish from the South China Sea. Science of the Total Environment, 677: 493–501

Zhou Q, Zhang H, Fu C, Zhou Y, Dai Z, Li Y, Tu C, Luo Y (2018). The distribution and morphology of microplastics in coastal soils adjacent to the Bohai Sea and the Yellow Sea. Geoderma, 322: 201–208

Ziajahromi S, Kumar A, Neale P A, Leusch F D (2018). Environmentally relevant concentrations of polyethylene microplastics negatively impact the survival, growth and emergence of sediment-dwelling invertebrates. Environmental Pollution, 236: 425–431

Zobkov M, Esiukova E (2017). Microplastics in Baltic bottom sediments: Quantification procedures and first results. Marine Pollution Bulletin, 114(2): 724–732